Regional estimation of savanna grass nitrogen using the red-edge band of the RapidEye sensor

Ramoelo A.[a, b,*], Skidmore A.K[b]., Cho M.A[a]., Schlerf M[b]., Mathieu R[a]., Heitkönig I.M.A[c].

[a]Earth Observation Research Group, Natural Resource and the Environment Unit, Council for Scientific and Industrial Research (CSIR), P.O.Box 395, Pretoria, 0001, South Africa
[b]Faculty of Geoinformation Science and Earth Observation, University of Twente (UT-ITC), P.O.Box 217, 7500 AE Enschede, The Netherlands
[c]Resource Ecology Group, Wageningen University, Droevendaalsesteeg 3a, 6708 PB Wageningen, The Netherlands

*Corresponding Author: Abel Ramoelo, Tel: +2712 841 3840, Fax: +2712 841 3909, Email: aramoelo@csir.co.za or ramo14741@itc.nl

Abstract

The regional mapping of grass nutrients is of interest in the sustainable planning and management of livestock and wildlife grazing. The objective of this study was to estimate and map foliar and canopy Nitrogen (N) at a regional scale using a recent high resolution spaceborne multispectral sensor (i.e. RapidEye) in the Kruger National Park (KNP) and its surrounding areas, South Africa. The RapidEye sensor contains five spectral bands in the visible-to-near infrared (VNIR), including a red-edge band centered at 710 nm. The importance of the red-edge band for estimating foliar chlorophyll and N concentrations has been demonstrated in many previous studies, mostly using field spectroscopy. The utility of the red-edge band of the RapidEye sensor for estimating grass N was investigated in this study. A two-step approach was adopted involving (i) vegetation indices and (ii) the integration of vegetation indices with environmental or ancillary variables using a stepwise multiple linear regression (SMLR) and a non-linear spatial least squares regression (PLSR). To ensure that the estimation of grass N was not compromised by biomass variability, the field work was undertaken during peak productivity. The model involving the simple ratio (SR) index (R_{805}/R_{710}) defined as SR54, altitude and the interaction between SR54 and altitude (SR54*altitude) yielded the highest accuracy for canopy N estimation, while the non-linear PLSR yielded the highest accuracy for foliar N estimation through the integration of remote sensing (SR54) and environmental variables. The spatial pattern of foliar N concentrations corresponded with the soil fertility gradient induced by the geological parent material. The study demonstrated the possibility to map grass nutrients at a regional scale provided there is a spaceborne sensor encompassing the red edge waveband with a high spatial resolution. Regional maps of the grass nutrients could be used for planning and management of the savanna ecosystems by farmers, resource managers and land use planners.

Keywords: foliar nitrogen, savanna ecosystem, integrated modeling, red-edge band, RapidEye, vegetation indices

1. Introduction

Savanna ecosystems constitute about 32.8% of the land in South Africa (Mucina and Rutherford, 2006). These ecosystems play a crucial role in the rural economy of the country, and worldwide as well (James et al., 2003; Shackleton et al., 2002). Among other things, they provide grazing resources important for livestock production, one of the main sources of income in South African rural areas (Shackleton et al., 2002). The main challenge for savannas is their sensitivity to land degradation due to overgrazing and overstocking (Abel and Blaikie, 1989; Du Toit and Cumming, 1999; Everson and Hatch, 1999). This is at least in part the result of the lack of information about grass conditions hampering proper management (Everson and Hatch, 1999). There is a need for sustainable utilization of the grazing land for viable livestock production, while minimizing land degradation. Spatial and regional information about grass nutrients is useful to guide farmers towards sustainable management of their grazing land, thus alleviating poverty.

Regional mapping of grass nitrogen (N) provides essential information for sustainable planning and management of livestock and wildlife grazing by livestock farmers, park wardens, or game and resource managers. Grass N concentration is an indicator of grass quality as it is positively correlated to protein content (Clifton et al., 1994; Wang et al., 2004). Protein forms one of the major nutrient requirements for herbivores (Prins and Beekman, 1989; Prins and van Langevelde, 2008). Grass quality is an important parameter affecting the distribution and grazing behaviour of livestock and wildlife (Ben-Shahar and Coe, 1992; Heitkönig and Owen-Smith, 1998; McNaughton, 1990). For example, large herbivores concentrate in highly nutritious areas in southern Africa (Grant and Scholes, 2006; Owen-Smith and Danckwerts, 1997; Treydte et al., 2007) and herbivore diversity increases with increasing soil fertility levels (Olff et al., 2002). Soil fertility levels generally correlate with grass N concentrations (Ben-Shahar and Coe, 1992; Olff et al., 2002). Therefore, grass N concentrations could be used as a proxy for soil fertility levels.

Remote sensing techniques have been developed over the past decades to extract information about biophysical and biochemical parameters of vegetation such as leaf area index, chlorophyll, P, fibre, lignin, and N (Asner et al., 1998; Beeri et al., 2007; Darvishzadeh et al., 2008; LaCapra et al., 1996; Main et al., 2011; Majeke et al., 2008; Ramoelo et al., 2011b; Schlerf et al., 2010). The conventional approach relates a specific vegetation parameter to vegetation indices derived from remote sensing data using a variety of statistical regression techniques (Darvishzadeh et al., 2008; Haboudane et al., 2004; Hansen and Schjoerring, 2003; le Maire et al., 2008; Starks et al., 2008). For estimating foliar biochemical (e.g. N) concentrations, traditional broadband indices such as normalized difference vegetation index (NDVI) (Rouse et al., 1974), soil line concept (SLC), simple ratio (SR) (Baret and Guyot, 1991), and soil-adjusted vegetation index (SAVI) (Huete, 1988) are not conducive. These broadband vegetation indices saturate at high canopy cover (Mutanga and Skidmore, 2004b; Tucker, 1977) and are insensitive to subtle changes in the foliar N concentration.

The more recent success in estimating foliar N and chlorophyll concentrations has been possible due to the development of hyperspectral remote sensing. Studies using hyperspectral remote sensing have highlighted the utility of red-edge bands for estimating foliar N and chlorophyll concentrations (Cho and Skidmore, 2006; Darvishzadeh et al., 2008; Huang et al., 2004). The red-edge is the region of abrupt change in leaf reflectance between 680 and 780 nm, mainly influenced by the concerted effect of spectral absorption in the red wavelengths and scattering in the near infrared region (Clevers et al., 2002; Gates et al., 1965; Horler et al., 1983). Cho and Skidmore (2006) developed a technique to compute the red-edge position (REP), which is highly sensitive to foliar chlorophyll. REP is known to be insensitive to background effects (Elvidge and Chen, 1995) and is highly correlated to foliar N (Cho and Skidmore, 2006), as chlorophyll is positively correlated to N (Haboudane et al., 2004; Hansen and Schjoerring, 2003; Yoder and Pettigrew-Crosby, 1995). Vegetation indices computed from red-edge bands, also known as narrow-band indices, have provided improved estimates of foliar N compared to conventional broad-band indices derived from red (680 nm) and near infrared (800 nm) (Hansen and Schjoerring, 2003; Mutanga and Skidmore, 2007).

Other successful hyperspectral techniques in foliar N estimation involve the use of N and protein absorption features in the visible (VIS), near infrared (NIR) and shortwave infrared (SWIR) (Huang et al., 2004; Knox et al., 2010; Schlerf et al., 2010; Skidmore et al., 2010). Several studies argued that the use of selected absorption features surpasses the use of the full spectrum for foliar biochemical and biophysical estimation (Cho et al., 2007; Darvishzadeh et al., 2008), because it reduces the chance of using redundant data. The drawback to using this approach for regional estimation of foliar biochemical concentrations is that there are limited satellite sensors which sample light using the full spectral region with narrow bands adequately resolving these absorption features. Satellite sensors with strategically placed spectral bands in the red-edge region are likely to provide successful estimates of biochemical concentrations, and more specifically N. However, as these sensors are scarce, foliar N concentration is seldom mapped on a regional scale. For example, conventional multispectral satellite sensors such as SPOT, Landsat, and ASTER lack specific spectral bands in the red-edge region and their spatial resolutions are relatively coarse. The MERIS sensor has a standard band setting allowing the computation and approximation of the red-edge position (Clevers et al., 2002), but the spatial resolution is too coarse, especially for savannas, which are a complex and heterogeneous mosaic of grass and trees. The emergence of multispectral sensors such as WorldView-2 (USA), SumbandilaSAT (South Africa) and RapidEye (Germany) with red-edge bands at high spatial resolution (i.e. 6.5 m) could provide an opportunity for rangeland resource quality assessment at a regional level. There is a need for the development of specific vegetation indices that could be used successfully with these sensors. In this study several broad-band and hyperspectral vegetation indices were modified to incorporate the red-edge band of RapidEye to estimate grass N concentration at a regional scale.

A challenge when using remote sensing to estimate foliar biochemical concentrations is associated with the difficulty disentangling the signals for biomass and foliar biochemical concentrations, especially N (i.e. the interaction effects between N and biomass) (Skidmore et al., 2010). These effects can be minimized during peak productivity when the grass spectra have the highest absorption in the red region and scattering in the near infrared region (Plummer, 1988a, b; Skidmore et al., 2010). During this period, the scattering and absorption processes continue to increase due to biomass production, as captured by indices such as normalized difference vegetation index (NDVI), and the relationship between biomass and NDVI asymptotically saturates (Mutanga and Skidmore, 2004b; Tucker, 1977). At a certain critical biomass point (e.g. 0.3 g/cm^2) reached at peak productivity, the vegetation indices are unable to estimate further increase in biomass (Mutanga and Skidmore, 2004b). That is when foliar N can be estimated with minimal effect from the N-biomass interaction problem.

In addition, a few studies have highlighted the need to integrate environmental or ancillary and remote sensing variables to estimate foliar biochemical concentrations at a regional scale (Cho et al., 2009; Cho et al., 2010; Knox et al., 2011; Ramoelo et al., 2011a; Ramoelo et al., *under review*), which could be a crucial step towards improving regional estimation and mapping. A combination of factors such as edaphic (geology and soils), topographic (slope, aspect, and altitude), and climatic (precipitation and temperature) factors are known to influence the distribution of foliar biochemical concentrations in a very complex way (Ben-Shahar and Coe, 1992; Ferwerda et al., 2006; Mutanga et al., 2004; Skidmore et al., 2011). Ramoelo et al. (2011a) showed that geology, slope, temperature, and land use types were the main contributing environmental variables when modeling foliar N in combination with *in situ* hyperspectral remote sensing variables. However, where environmental data sets are readily available at a regional scale, their resolution is relatively coarse rendering them unsuitable as sole input in the estimation of foliar biochemical concentrations. The use of remote sensing could address this issue of resolution and scale, for instance regional maps could be derived at a resolution of 5 to 10 m based on data from the newly developed spaceborne sensors. The assumption is that a modeling approach which integrates remote sensing and environmental variables potentially yields a higher foliar N estimation accuracy than approaches using either remote sensing or environmental variables (Cho et al., 2009; Cho et al., 2010; Knox et al., 2011; Ramoelo et al., 2011a; Ramoelo et al., *under review*). The objectives of this study were twofold; (1) to investigate the utility of the red-edge band of the RapidEye sensor for estimating grass N concentrations using various vegetation indices derived from the RapidEye data, and to determine which vegetation index correlates highly with grass foliar as well as canopy N and (2) to integrate this vegetation index with the environmental variables to estimate and map grass foliar and canopy N at a regional scale.

2. Study area

The study area is located in the north-eastern part of South Africa (Figure 1) and covers a total area of approximately 5000 km². The area is referred to as the Lowveld landscape, which is a low lying area extending from the foot slopes of the Drakensberg Great Escarpment to the west to the Mozambique coastal plain to the east (Venter et al., 2003). Protected areas such as the privately owned Sabi Sands Game Reserve (SGR) and the state -owned Kruger National Park (KNP), as well as the communal lands in Bushbuckridge form the main land tenures. The main vegetation types are “Tshokwane-Hlane basalt lowveld”, “granite lowveld”, “gabbro grassy bushveld”, and “Delagoa lowveld” (Mucina and Rutherford, 2006). The Tshokwane-Hlane basalt lowveld is characterized by open tree savannas with trees such as *Sclerocarya birrea, Acacia nigrescens*, *Acacia gerrardii, Peltophorum africanum, Dichrostachys cinerea,* and common grass species such as *Bothriochloa radicans, Digitaria eriantha, Cenchrus ciliaris,* and *Urochloa mossambicensis.* This vegetation type occurs in the highly fertile black, brown or red clayey soils derived from the basalt substrate. The granite lowveld comprises dense thickets dominated by trees such as several *Combretum* species, *Dichrostachys cinerea*, *Grewia bicolor,* and *Terminalia sericea* with dominant grass species being *Pogonarthria squarrosa, Tracholeona monachne*, and *Eragrostis rigidior.* The granite-derived soils are sandy in the uplands and clayey in the bottomlands, and are low in fertility compared to the basalt-derived soils. Gabbro grassy bushveld constitutes an open savanna with dense grass cover. Dominant tree species are *Acacia nigrescens*, *Sclerocarya birrea, Bolusanthus speciosus,* and *Ziziphus mucronata*, while common grass species are *Chloris virgata, Setaria species, Themenda triandra*, *Bothriochloa radicans, Panicum maximum, Urochloa mossambicensis,* and *Eragrostis superba*. Soils in this vegetation type are fertile dark vertic with 20 to 50% clay derived from the gabbro geological type (Mucina and Rutherford, 2006). The Delagoa lowveld vegetation type is characterized by dense thickets with common tree species such as *Acacia welwitschii, Dichrostachys cinerea*, *Euclea divinorum,* and *Grewia bicolor* and grass species such as *Chloris virgata, Aristida congesta, Panicum colaratum,* and *Sporobolus* species. This vegetation type occurs in shale and lesser sandstone layers interspersed by sheets and dykes of Jurassic dolerite (Mucina and Rutherford, 2006). The soils are rich in sodium, but the fertility is lower than in the basaltic-derived soils. There is an evident precipitation gradient from the western part (800 mm/year) to the eastern part (580 mm/year) of the study area (Venter et al., 2003). The annual mean temperature is about 22^{o}C. Geology as mentioned above includes granite and gneiss with local intrusions of gabbro in the west and basalt as well as shale in the eastern part towards Mozambique (Venter et al., 2003). The contrasting geological substrates (and associated soil types) together with the precipitation influence, clearly define the patterns and gradients in soil moisture and nutrients. The topography is mostly undulating in the granitic sites and flat in the basalt areas, with an average height of 450 m. Rangelands in the protected areas are grazed by wild herbivores such as impala (*Aepyceros melampus*), zebra (*Equus burchelli*), wildebeest (*Connochaetes taurinus*), and buffalo (*Syncerus caffer*), while the communal rangelands support the grazing of cattle (*Bos taurus*), goats (*Capra hircus*), and sheep (*Ovis aries*), thus determining various grazing or land use intensities.

3. Data Collection

3.1. Field data collection

The field data were collected using a road sampling technique since deep penetration into the savanna landscape was limited by management and logistical restrictions. Field work was undertaken in April 2010, the same month the satellite imagery was collected. The areas along the main roads covering the study area were purposively selected for the field sampling based on their underlying geological strata, both in the protected and in the communal areas. Buffers of 300 m were created on both sides of these roads using ArcGIS software (ESRI, USA). Within the buffer polygons random sample points were generated using the ArcGIS add-on called Hawth tools. All points directly on the road or on the bare areas next to the road were rejected because of the lack of grass. The plots were randomly located in areas with homogeneous grass to avoid the effect of trees on the grass signal. Each sample point (N=51) was treated as a plot of 20 m x 20 m, to account for a geometric accuracy of up to one pixel (i.e. 5 m) on the RapidEye image. In each plot, 2 subplots of 50 cm x 50 cm were used to collect information about the dominant species, the percentage cover of photosynthetic and non-photosynthetic vegetation as well as bare soil. The grass in each subplot was clipped and weighed to determine the wet biomass. The grass samples were then dried at 80ºC for 24 hours and weighed again to establish the dry biomass. Grass biomass was expressed in weight per unit area (i.e. g/0.25 m^2). The biomass data were acquired to determine any interaction effects between biomass and foliar N. The field work was undertaken during peak productivity to minimize these interaction effects (Plummer, 1988a, b; Skidmore et al., 2010), as discussed in the Introduction. The grass samples were dried to retrieve foliar N concentrations.

3.2. Chemical analysis

The dried grass samples were taken to South Africa’s Agricultural Research Council Institute for Tropical and Subtropical Crops (ARC-ITSC) in Nelspruit for chemical analysis. Firstly, the acid digestion technique was used, where sulphuric acid aided the foliar N retrieval (Giron, 1973; Grasshoff et al., 1983; Mutanga et al., 2004). Secondly, the colorimetric method by auto analyser was used to measure the foliar N (Technicon Industrial Method 329-74 W; Technicon Industrial Systems, Farrytown, New York). An emerald-green colour was formed by the reaction between ammonia, sodium salicylate, sodium nitroprusside, and sodium hypochlorite. The ammonia-salicylate complex was read at 640 nm. These two extraction methods were already successfully used for grass foliar N by Mutanga et al. (2004), Ramoelo et al. (2011b) and Ramoelo et al. (*under review*).

3.3. Image acquisition and atmospheric corrections

The mission to collect RapidEye images was tasked in April 2010. The RapidEye sensor has a multispectral push broom imager with a spatial resolution of 6.25 m and captures data in the spectral bands: blue(440-550 nm), green (520-590 nm), red (630-685 nm), red edge (690-730 nm), and near infrared (760-850 nm) (RapidEye, 2010). The RapidEye Ortho product (Level 3A) was provided with radiometric, sensor, and geometric correction applied using the digital terrain elevation data (DTED) level 1 Shuttle Radar Terrain Mission (SRTM). The orthorectification accuracy of 1 or less pixel was achieved (RapidEye, 2010). The RapidEye Ortho product was delivered resampled to a 5m x 5m spatial resolution. To retrieve surface reflectance atmospheric correction was executed using the atmospheric and topographic correction software (ATCOR 2) implemented in the IDL Virtual Machine (Richter, 2011). ATCOR 2 models reflectance for flat surfaces, which was considered sufficient since the study area was not characterized by very rugged terrain. The advantage of ATCOR 2 is that it was developed specifically for satellite remote sensing data and includes a large database of atmospheric correction functions (look-up-tables computed with the Modtran® 5 radiative transfer code) covering a wide range of weather conditions, sun angles, and ground elevations (Richter, 2011). The Modtran® standard aerosols for “rural” were selected to compute the aerosol type, and “visibility” was computed according to Richter (2011). RapidEye metadata were used to obtain additional important information for reflectance retrieval such as satellite and solar zenith angle, satellite and solar azimuth angle, as well as relative azimuth angle. The workflow for implementing ATCOR for atmospheric correction in any terrain is well outlined in Richter (2011).

3.4. Environmental or ancillary variables

Several studies showed that climate, topography, and geologic substrate influence the distribution of primary environmental regimes such as moisture and nutrients in soils or plants; for details see the review by Skidmore et al. (2011), as well as Pickett et al. (2003), Venter et al. (2003) and Mutanga et al. (2004). Several environmental variables influence the distribution of grass N at different scales; these include precipitation, temperature, land use, geology, soils, distance to rivers, altitude, slope, and aspect (Table 1). Mean annual precipitation (MAP) and temperature (MAT) were acquired from the World Climate database (WorldClim) (www.WorldClim.com). This climatic database has been widely used for biodiversity and ecological applications (Hijmans et al., 2001) and climatic stations are spread across South Africa (Adams and Church, 2007; Hijmans et al., 2005; Saad et al., 2007). The freely available SRTM 4.1 Digital Elevation Model (DEM) with its relatively high spatial resolution of 90 m (Javis et al., 2008) was used. To make it more reliable, Javis et al. (2008) further improved the DEM by filling in the holes identified. Slope and aspect were derived from the DEM using ArcGIS 10x. The river layer was sourced from the South African National Botanical Institute (SANBI)'s Beta version of vegetation data sets (Mucina and Rutherford, 2006). The 'distance to river' variable was computed using the Spatial Analyst Tool embedded in ArcGIS 10x, where the river layer and the sample plot locations (GPS points) formed the inputs. A soil layer was acquired from the soil and terrain database of Southern Africa (SOTERSAF) (Dijkshoorn, 2003) (Table 1). This soil map has been used for the Land Degradation Assessment in Drylands project (LADA), for which South Africa is one of the partners (Dijkshoorn et al., 2008). The land use types were derived from the boundary layers of KNP, Sabi Sands Game Reserve and the communal areas, acquired from KNP's Geographic Information System (GIS) and remote sensing laboratory.

(Table 1)

4. Data Analysis

The reflectance data corresponding to each field plot were extracted from the image in order to perform the statistical analysis. The vegetation indices listed in Table 2 were computed from the extracted reflectance data. The new or modified vegetation indices were mainly developed to benefit from the inclusion of the red-edge band in the RapidEye spectral configuration. In Table 2, simple ratios (SRs) are written as SR53, 54, and 43, just as the normalized difference vegetation indices (NDVIs) are written as NDVI54 and so on, denoting the band combinations used. In some cases, such as plant pigment ratio (PPR), transformed chlorophyll absorption index (TCARI), and modified chlorophyll absorption index (MCARI), the indices were given new RapidEye compatible bands less than 60 nm from the original indices, to ensure that the sensitivity of the specific region of the spectrum was maintained. All the indices selected were sensitive to leaf and canopy chlorophyll (Table 2). For statistical analysis, the foliar N concentration was multiplied by the percentage cover of photosynthetic vegetation (PV) to derive a unit-less canopy integrated nitrogen content, denoted as N*PV (He and Mui, 2010; Wessman, 1992).

(Table 2)

4.1. Univariate and Multivariate analysis

The univariate analysis involved bootstrapping the linear regression between biochemical (foliar and canopy N) and vegetation indices. Subsequently, the results from that analysis were used to select the vegetation index, based on a high coefficient of determination (R^2) and a low root mean square error (RMSE) (Bunke and Droge, 1984; Efron and Tibshirani, 1997; Fox, 2002; Fox and Weisberg, 2010). The multivariate analysis was undertaken using an integrated modeling approach. The vegetation index (with a high estimation accuracy resulting from bootstrapping statistics combined with environmental variables) was used to predict N concentrations. The first multivariate analysis was performed using a combination of principal component analysis (PCA) and stepwise multiple linear regression (SMLR) (Çamdevýren et al., 2005), denoted as SMLR+PCA. The aim of the PCA was to decompose the independent variables into uncorrelated components. The advantage of the PCA was that it reduced multicollinearity and overfitting (Çamdevýren et al., 2005; Jain et al., 2007). In this approach, the initial step was to run the PCA on the independent variables, i.e. the vegetation index and environmental variables. The second step was to run a forward stepwise regression to see which principal components (PC) significantly contributed to the N prediction model. The stepwise model was selected based on the lowest Akaike Information Criterion (AIC) (An and Gu, 1989; Sakamoto et al., 1986). The second multivariate analysis was performed using SMLR based on SR54 and environmental parameters (SMLR+Raw), where the model for predicting foliar N with high accuracy was selected using AIC, similar to the PCA+SMLR method. In this case the original data, i.e. highest performing vegetation index and environmental variables, were used for predicting N. Thirdly, the interaction effects between the selected variables for predicting foliar and canopy N at a SMLR+Raw stage were also tested using SMLR, and denoted SMLR+Raw+Int. Where the interaction effect between the significant variables selected according to lowest AIC improved the estimation accuracy for foliar and canopy N, this was reported, otherwise it was not reported. The final multivariate analysis was based on the non-linear partial least square regression (PLSR), and is known as PLSR with radial basis function

(RBF-PLSR). This non-linear PLSR was found to achieve a higher foliar N estimation accuracy than the conventional PLSR (Ramoelo et al., *under review*). This was mainly attributed to the fact that the non-linear PLSR has the combined capabilities of the conventional PLSR and an artificial neural network, maximizing covariance between data sets and non-linear model fitting (Walczak and Massart, 1996). The initial stage of applying this technique was to standardize the data sets to within a range of 0 to 1 (Knox et al., 2011; Ramoelo et al., *under review*). Sigma values were specified in order to compute the activation matrix using the radial basis function. The activation matrix was then used in combination with PLSR to predict foliar N concentrations, with the number of uncorrelated latent variables or factors specified.

4.2. Validation

Validation was performed using a bootstrapping technique because of the small sample sizes involved (Bunke and Droge, 1984; Efron and Tibshirani, 1997). Bootstrapping is an unbiased way to validate models as it has an iteration component. It samples the data a number of times, which makes it a more robust way of validating models, as well as extremely efficient when only few samples are collected. In this study we used 1000 iterations to ensure that the bias was highly reduced. The highly accurate bootstrapped model was inverted and applied to the RapidEye image to map the predicted foliar and canopy N concentrations of the grass canopies. The validation of the non-linear PLSR was based on a Monte-Carlo cross validation, since bootstrapping was not yet incorporated in the TOMCAT software (Walczak and Massart, 1996).

4.3. Descriptive and exploratory analysis

One-way analysis of variance (ANOVA) was computed to test if there was any significant difference between foliar N and, firstly, geology and, secondly, soils. The Spearman's rank correlation was used to quantify the relationship between remote sensing and environmental variables, since it can be applied to both categorical and continuous data (Lehman, 1998). The descriptive statistics, i.e. the mean, minimum and maximum, as well as standard deviation values of N and N*PV were computed using the R programming language.

5. Results

5.1. Determining the vegetation index with a high N estimation accuracy

The SR54 computed with the red-edge band yielded the highest accuracy for predicting both foliar and canopy N; surpassing the results of the conventional simple ratio (i.e. SR53) (Table 3, Figures 2 and 3). At foliar level, the bootstrapped model resulted in R^2=0.23 and RMSE=0.15029%, while at canopy level, the bootstrapped model resulted in R^2=0.45 and RMSE=13.50580 (unit-less). Of the twenty four indices used to estimate foliar and canopy N, the inclusion of the newly embedded red-edge band in the RapidEye data improved the results especially for the top five indices, i.e. SR54, NDVI54, SAVI, OSAVI, and SIPI1 for canopy N, and SR54, NDVI54, OSAVI, SAVI, and MTCI for foliar N concentrations (Table 3, Figures 2 and 3). Generally, there are five indices that could be directly modified to make use of the red-edge band rather than relying on the conventional versions using red and NIR bands, namely SR, NDVI, SAVI, OSAVI, and SIPI. The least performing indices were TVI, TCARI, and MCARI with RMSEs of between 17.3641 and 18.1006 for canopy N and between 0.1704 and 0.1713% for foliar N. The variance in canopy N was explained more clearly by the vegetation indices than the variance in foliar N was, with the R^2 increasing from 0.23 for foliar to 0.45 for canopy N. A similar pattern was evident in the estimation accuracy measured according to RMSE (Table 3).

(Table 3)
(Figure 2)
(Figure 3)

5.2. Integrated modeling for grass N prediction

Integrating vegetation indices and environmental variables for estimating canopy N using SMLR (SMLR+Raw+int) yielded a significantly higher estimation accuracy (bootstrapped: R^2=0.64, RMSE=11%; 17% of the mean), than the model using SR54, altitude, and SR54*altitude (Table 4). The non-linear PLSR (RBF-PLSR) was the second highest performer concerning the accuracy of estimating canopy N (bootstrapped: R^2=0.61, RMSE=11%), after SMLR, with interaction effects from SR54 and altitude (Table 4). As shown in Table 5, altitude is significantly correlated with other environmental variables such as geology, precipitation, temperature, slope, aspect, and land use. It is evident that altitude in this study is a proxy for various other environmental variables. The last technique tested was principal component analysis and regression (SMLR+PCA), which resulted in a lower canopy N estimation accuracy (bootstrapped: R^2=0.56, RMSE=12.33; 19% of the mean) than the above two techniques, with principal components (PC) 1, 3, and 9 selected (Table 4).

(Table 4)
(Table 5)

For the estimation of foliar N, the non-linear PLSR produced a significantly higher estimation accuracy (bootstrapped: R^2=0.48, RMSE=0.12%; 14% of the mean) than other techniques such as SMLR (Table 4). The SMLR+PCA yielded the second highest estimation accuracy (bootstrapped: R^2=0.45, RMSE=0.13%; 15% of the mean) and the least performing technique was the SMLR+Raw (bootstrapped: R^2=0.44, RMSE=0.14%; 17% of the mean) (Table 4). The interaction effects analysis of the selected variables in SMLR+Raw did not improve the results. Figure 4 shows the spatial distribution of foliar and canopy N at a regional scale. There is a clear N gradient between the western and the eastern part of the study area (Figure 4). The general pattern of foliar and canopy N follows the geological types, i.e. basalt and gabbro areas are characterized by more highly nutritious grass than the shale and granitic derived grasses (Figure 4).

(Figure 4)

5.2. Descriptive and exploratory statistics

The foliar N concentration across the study had a mean of 0.84%, as shown in Table 6. After converting the foliar N concentrations to the canopy integrated N using PV (i.e. N*PV), the recorded mean was 74.71 (Table 6). Foliar N concentrations varied significantly according to geology (F=3.1865, p=0.0322) and soil type (F=3.7871, p=0.0096), as was confirmed by the ANOVA.

(Table 6)

6. Discussion

The study investigated the utility of the red-edge band from the RapidEye sensor using vegetation indices, in order to determine which index correlated highly with foliar and canopy N. This index was then integrated with environmental variables to predict foliar and canopy N at a regional scale. SR54 was not only selected as the vegetation index with the highest predictive capability compared to other indices, it was also selected as a significant variable in the stepwise model successfully predicting both foliar and canopy N (Table 4). The performance of SR54 could be attributed to the use of red-edge waveband which contributed to the estimation of foliar N concentrations. Similar trends were observed for NDVI and SAVI, where the inclusion of the red-edge band improved the estimation results. The importance of the red-edge band is due to the fact that it is highly correlated to chlorophyll (Cho and Skidmore, 2006; Clevers et al., 2002) and insensitive to background effects (Zarco-Tejada et al., 2004). It is known that there is a positive correlation between chlorophyll and foliar N (Vos and Bom, 1993; Yoder and Pettigrew-Crosby, 1995). This study is consistent with the *in situ* hyperspectral remote sensing studies reported by Mutanga and Skidmore (2007), Gong et al. (2002), and Cho and Skidmore (2006). Additionally, the performance of SR has not only been demonstrated with the retrieval of foliar biochemicals but also for biophysical parameters such as leaf area index (Jiang et al., 2005; Darvishzadeh et al., 2008) and biomass (Mutanga and Skidmore, 2004b).

The integrated modeling approach has produced higher grass N accuracy results compared to univariate approaches using only vegetation indices. The advantage of using an integrated modeling approach for N estimation is that both remote sensing and environmental variables are considered. The use of environmental variables is generally constrained by the lack of detail in studies on a regional scale, rendering proper estimation of foliar N impossible. Remotely sensed imagery helps to provide the spatial detail important for characterizing foliar N in grass canopies. The combination of non-linear PLSR with environmental variables estimated foliar N with relatively high accuracy. The non-linear PLSR combined advantages of the conventional PLSR and an artificial neural network, i.e. maximizing the covariance between data sets and non-linear model fitting (Walczak and Massart, 1996). Additionally, the non-linear PLSR can be used with non-normal data.

Estimation of canopy N using SMLR integrating remote sensing (SR54) and environmental variables resulted in the highest estimation accuracy. SMLR selected SR54 and altitude, which predicted N with the lowest AIC value. Table 5 shows altitude to be significantly correlated with other environmental variables such as geology, mean annual precipitation, mean annual temperature, slope, aspect, and land use types. Soil and geology are also cited as factors which influence the distribution and concentrations of nutrients in grass (Mucina and Rutherford, 2006; Venter et al., 2003). Soils developed in basalts are generally high in nutrients, while the granitic soils are associated with low nutrient concentrations (Scholes et al., 2003; Venter et al., 2003). Grasses such as *Bothriochloa radicans*, *Urochloa mossambicensis*, and *Digitaria eriantha* are found dominating the basaltic-derived soils because of these high nutrient concentrations. These species also produce bigger leaves than the species usually found in the granitic-derived soils such as *Eragostris rigidior* and *Sporobolus* species. The bigger leaves potentially increase photosynthetic activity, and hence productivity. Table 5 shows a negative correlation between foliar N and precipitation. The western part of the study area is characterized by high precipitation and lower soil fertility-granite-derived soils, while the eastern part experiences low precipitation on high soil fertility-basaltic-derived soils. Precipitation plays a crucial role in dissolving organic matter for the uptake of minerals by plants (Pickett et al., 2003). Land use type, giving an indication of the practices or activities taking place in the study area, is important as it is related to mean annual precipitation. Land use types are characterized by a pronounced rainfall gradient, with the communal areas receiving more rainfall than the protected areas (SGR and KNP). In addition, land use activities generally affect the grass's response to differences in precipitation (Zhou et al., 2002). Altitude, aspect and slope influence the distribution of nutrient concentrations in grass through their effect on soil temperature and water run-off (Roberts, 1987). Steeper slopes normally have higher run-off leading to thin soil layers supporting less nutritious grass (Mutanga et al., 2004). While valleys or bottomlands, characterized by deep soils, are the recipients of run-off from the steeper slopes, allowing support of high quality grasses (Scholes et al., 2003).

Foliar N estimation results were low compared to the results for canopy N, for all methods. This is an indication that foliar N is not readily estimated by image spectra, which are largely dependent on canopy cover and properties (e.g. leaf area index). Canopy N, which can be accurately retrieved by image spectra, includes information about foliar N and structure or canopy productivity. The poorer results for foliar N, in comparison to the canopy N estimation, are consistent with other vegetation biochemical studies, including the ones focusing on foliar and canopy chlorophyll (Asner, 1998; Asner and Martin, 2008; Asner et al., 1998; Darvishzadeh et al., 2008; Yoder and Pettigrew-Crosby, 1995). These studies further demonstrated that there is poor propagation of light or signal from leaf to canopy.

In this study, the interaction effect between foliar N and biomass was minimized by conducting fieldwork and acquiring the RapidEye image during peak productivity in wet season (Figure 5). During this period, the relationship between biomass and vegetation indices is asymptotic, as portrayed in Figure 5. The amount of light that can be absorbed in the red region of the spectrum plateaus during peak productivity (Mutanga and Skidmore, 2004b; Thenkabail et al., 2000; Tucker, 1977). Additionally, the NIR reflectance continues to increase, because addition of new leaves influences the multiple scattering (Kumar et al., 2001). This result in slight changes in the vegetation index (e.g. NDVI), while causing a poor relationship with biomass. The concentration of foliar N, in particular, reaches a maximum during active growth in the wet season (Tolsma et al., 1987). Therefore, it is assumed that foliar N dominates the reflectance in times of maximum productivity, and that during this period foliar N can be successfully estimated (Skidmore et al., 2010).

(Figure 5)

In this study 60% of the variance of canopy N is attained using multispectral remote sensing data (i.e. RapidEye), which is comparable to some of the hyperspectral studies. The performance of the RapidEye data in estimating foliar and canopy N is associated with the presence of the red-edge band. The hyperspectral studies demonstrated the use of the red-edge position to estimate chlorophyll and N (Cho and Skidmore, 2006; Darvishzadeh et al., 2008). Foliar and canopy N were estimated because of the positive correlation between chlorophyll and N (Yoder and Pettigrew-Crosby, 1995). Previous studies using hyperspectral data (*in situ* or airborne) achieved high foliar N retrieval accuracies. Using airborne systems, foliar N estimation was reported to achieve accuracies of 48 to 80% (Huang et al., 2004; Knox et al., 2011; Mutanga and Skidmore, 2004a; Skidmore et al., 2010). An explained variance of 48% was obtained during the dry season, while 80% or more was obtained during the wet season. This shows the importance of seasonality or plant phenology in the estimation of foliar biochemical levels.

The results of this study demonstrated that foliar and canopy N can be mapped at a regional scale using spaceborne multispectral remote sensing data during times of peak productivity. The red-edge band of RapidEye was found to be important in achieving this goal (compared to traditional multispectral sensors such as SPOT and Landsat). Foliar N is an indicator of crude protein (Clifton et al., 1994; Wang et al., 2004), which forms a main nutrient requirement (Prins and van Langevelde, 2008), and could be used for understanding the distribution, densities and population dynamics of herbivores in protected and communal areas (Ben-Shahar and Coe, 1992; Heitkönig and Owen-Smith, 1998; McNaughton, 1988, 1990; Mutanga et al., 2003). Photosynthetic vegetation cover is one of the canopy parameters determining key ecosystem functions, e.g. rate of carbon and nutrient intake (Guerschman et al., 2009). In addition, grass canopy N have a structural component as it was derived in combination with photosynthetic vegetation cover. The grass structure is generally defined by biochemistry, architecture, morphology and species composition (Burke, 1997; Drescher et al., 2006a; Drescher et al., 2006b). The grass structure affects grazing behavior of the herbivores (Drescher et al., 2006b). Drescher et al., (2006b) postulated that grass structure affects cattle grazing behavior in the South African savanna. Therefore, canopy N may outperform foliar N when aiming to understand the distribution of herbivores, since it can be estimated and mapped at a higher accuracy. The study further demonstrated the use of integrated modeling for grass N estimation. Regional nutrient maps could provide useful information to farmers, resource managers and park stewardships for sound planning and management of savanna ecosystems.

7. Acknowledgement

We would like to thank the Council of Scientific and Industrial Research (CSIR), the University of Twente Faculty of Geoinformation Science and Earth Observation (UT-ITC), and Wageningen University for the funding provided. We would also like to acknowledge the South African Department of Science and Technology as well as National Research Foundation (NRF)'s Professional Development Programme (PDP) for the funding. We appreciated the field work assistance by Mr Thulani Selaule, as well as the involvement of South African National Parks (SANPARKS), especially Dr Izak Smith, Mrs Thembi Khoza, Mrs Patricia Khoza, Mr Adolf Manganyi, and Mrs Onica Sithole for making the fieldwork possible.

8. References

Abel, N.O.J., Blaikie, P.M., 1989. Land degradation, stocking rates and conservation policies in the communal rangelands of Botswana and Zimbabwe. Land Degradation and Rehabilitation 1(2), 101-123.

Adams, D.C., Church, J.O., 2007. Amphibians do nor follow Bergmann's rule. Evolution 62-2, 413-420.

An, H., Gu, L., 1989. Fast stepwise procedures of selection of variables by using AIC and BIC criteria. Acta Mathematicae Applicatae Sinica (English Series) 5(1), 60-67.

Asner, G.P., 1998. Biophysical and Biochemical Sources of Variability in Canopy Reflectance. Remote Sensing of Environment 64(3), 234-253.

Asner, G.P., Martin, R.E., 2008. Spectral and chemical analysis of tropical forests: Scaling from leaf to canopy levels. Remote Sensing of Environment 112(10), 3958-3970.

Asner, G.P., Wessman, C.A., Schimel, D.S., Archer, S., 1998. Variability in Leaf and Litter Optical Properties: Implications for BRDF Model Inversions Using AVHRR, MODIS, and MISR. Remote Sensing of Environment 63(3), 243-257.

Baret, F., Guyot, G., 1991. Potentials and limits of vegetation indices for LAI and APAR assessment. Remote Sensing of Environment 35(2-3), 161-173.

Beeri, O., Phillips, R., Hendrickson, J., Frank, A.B., Kronberg, S., 2007. Estimating forage quantity and quality using aerial hyperspectral imagery for northern mixed-grass prairie. Remote Sensing of Environment 110(2), 216-225.

Ben-Shahar, R., Coe, M.J., 1992. The relationships between soil factors, grass nutrients and the foraging behaviour of wildebeest and zebra. Oecologia 90(3), 422-428.

Broge, N. H. & Leblanc, E. 2000. Comparing prediction power and stability of broadband and hyperspectral vegetation indices for estimation of green leaf area index and canopy chlorophyll density. Remote Sensing of Environment, 76 (2), 156-172.

Bunke, O., Droge, B., 1984. Bootstrap and Cross-Validation Estimates of the Prediction Error for Linear Regression Models. The Annals of Statistics 12(4), 1400-1424.

Burke, A., 1997. The impact of large herbivores on floral composition and vegetation structure in the Naukluft Mountains, Namibia. Biodiversity and Conservation 6(9), 1203-1217.

Çamdevýren, H., Demýr, N., Kanik, A., Keskýn, S., 2005. Use of principal component scores in multiple linear regression models for prediction of Chlorophyll-a in reservoirs. Ecol. Model. 181(4), 581-589.

Cho, M., Skidmore, A.K., Corsi, F., van Wieren, S., Sobhan, I., 2007. Estimation of green grass/herb biomass from airborne hyperspectral imagery using spectral indices and partial least square regressions. International Journal of Applied Earth Observation and Geoinformation 9(4), 414-424.

Cho, M.A., Skidmore, A.K., 2006. A new technique for extracting the red edge position from hyperspectral data: The linear extrapolation method. Remote Sensing of Environment 101(2), 181-193.

Cho, M.A., Van Aardt, J., Main, R., Majeke, B., Ramoelo, A., Mathieu, R., Norris-Rogers, M., Du Plessis, R., 2009. Integrating remote sensing and ancillary data for regional ecosystem assessment: Eucalyptus grandis agrosystem in Kwazulu Natal, South Africa, IEEE International Geoscience and Remote Sensing Symposium (IGARSS), Cape Town, South Africa, pp. 264-267.

Cho, M.A., Van Aardt, J.A.N., Main, R., Majeke, B., 2010. Evaluating variations of physiology-based hyperspectral features along a soil water gradient in a *Eucalyptus grandis* plantation. International Journal of Remote Sensing 31(16), 4507 - 4507.

Clevers, J.G.P.W., De Jong, S.M., Epema, G.F., Van Der Meer, F.D., Bakker, W.H., Skidmore, A.K., Scholte, K.H., 2002. Derivation of the red edge index using the MERIS standard band setting. International Journal of Remote Sensing 23(16), 3169 - 3184.

Clifton, K.E., Bradbury, J.W., Vehrencamp, S.L., 1994. The fine-scale mapping of grassland protein densities. Grass and Forage Science. 49(1), 1-8.

Darvishzadeh, R., Skidmore, A., Schlerf, M., Atzberger, C., Corsi, F., Cho, M., 2008. LAI and chlorophyll estimation for a heterogeneous grassland using hyperspectral measurements. ISPRS Journal of Photogrammetry and Remote Sensing 63(4), 409-426.

Dash, J. & Curran, P. J. 2004. The MERIS terrestrial chlorophyll index. International Journal of Remote Sensing, 25 (23), 5403 - 5413.

Daughtry, C. S. T., Walthall, C. L., Kim, M. S., De Colstoun, E. B. & Mcmurtrey, J. E. 2000. Estimating Corn Leaf Chlorophyll Concentration from Leaf and Canopy Reflectance. Remote Sensing of Environment, 74 (2), 229-239.

Dijkshoorn, K., 2003. SOTER database for Southern Africa (SOTERSAF): Technical Report. Internatioal Institute for Soil Reference and Information Centre, Wageningen.

Drescher, M., Heitkönig, I.M.A., Raats, J.G., Prins, H.H.T., 2006a. The role of grass stems as structural foraging deterrents and their effects on the foraging behaviour of cattle. Applied Animal Behaviour Science 101(1-2), 10-26.

Drescher, M., HeitkÖNig, I.M.A., Van Den Brink, P.J., Prins, H.H.T., 2006b. Effects of sward structure on herbivore foraging behaviour in a South African savanna: An investigation of the forage maturation hypothesis. Austral Ecology 31(1), 76-87.

Du Toit, J.T., Cumming, D.H.M., 1999. Functional significance of ungulate diversity in African savannas and the ecological implications of the spread of pastoralism. Biodiversity and Conservation 8, 1643-1661.

Efron, B., Tibshirani, R., 1997. Improvements on Cross-Validation: The .632+ Bootstrap Method. Journal of the American Statistical Association 92(438), 548-560.

Elvidge, C.D., Chen, Z., 1995. Comparison of broad-band and narrow band red and near-infrared vegetation indices. Remote Sensing of Environment 54(1), 38-48.

Everson, T.M., Hatch, G.P., 1999. Managing Veld (Rangelands) in the Communal Areas of Southern Africa, In: Tainton, N.M. (Ed.), Veld Management in South Africa. University of Natal Press, Pietermaritzburg.

Ferwerda, J.G., Siderius, W., Van Wieren, S.E., Grant, C.C., Peel, M., Skidmore, A.K., Prins, H.H.T., 2006. Parent material and fire as principle drivers of foliage quality in woody plants. Forest Ecology and Management 231(1-3), 178-183.

Fox, J., 2002. Bootstrapping regression models. Appendix to An R and S-PLUS Companion to Applied Regression http://cran.r-project.org/doc/contrib/Fox-Companion/appendix-bootstrapping.pdf , Accessed January 2011.

Fox, J., Weisberg, S., 2010. Bootstrapping Regression Models in R. An Appendix to An R Companion to Applied Regression, Second Edition http://socserv.mcmaster.ca/jfox/Books/Companion/appendix/Appendix-Bootstrapping.pdf , Accessed May 2011.

Gates, D.M., Keegan, H.J., Schleter, J.C., Weidner, V.R., 1965. Spectral properties of plants. Applied Optics 4(1), 11-20.

Giron, H.C., 1973. Comparison between dry ashing and wet digestion in preparation of plant material for atomic absorption analysis. Atomic Absorption Newsletter 12(1), 28-29.

Gitelson, A. A., Kaufman, Y. J. & Merzlyak, M. N. 1996. Use of a green channel in remote sensing of global vegetation from EOS-MODIS. Remote Sensing of Environment, 58 (3), 289-298.

Grant, C.C., Scholes, M.C., 2006. The importance of nutrient hot-spots in the conservation and management of large wild mammalian herbivores in semi-arid savannas. Biological Conservation 130(3), 426-437.

Grasshoff, K., Erhardt, M., Kremling, K., 1983. Methods of seawater analysis. Verlag Cheime, Weinhein, Germany.

Guerschman, J.P., Hill, M.J., Renzullo, L.J., Barrett, D.J., Marks, A.S., Botha, E.J., 2009. Estimating fractional cover of photosynthetic vegetation, non-photosynthetic vegetation and bare soil in the Australian tropical savanna region upscaling the EO-1 Hyperion and MODIS sensors. Remote Sensing of Environment 113(5), 928-945.

Haboudane, D., John, R., Millera, J. R., Tremblay, N., Zarco-Tejada, P. J. & Dextraze, L. 2002. Integrated narrow-band vegetation indices for prediction of crop chlorophyll content for application to precision agriculture. Remote Sensing of Environment, 81 (2-3), 416-426.

Haboudane, D., Miller, J.R., Pattey, E., Zarco-Tejada, P.J., Strachan, I.B., 2004. Hyperspectral vegetation indices and novel algorithms for predicting green LAI of crop canopies: Modeling and validation in the context of precision agriculture. Remote Sensing of Environment 90(3), 337-352.

Hansen, P.M., Schjoerring, J.K., 2003. Reflectance measurement of canopy biomass and nitrogen status in wheat crops using normalized difference vegetation indices and partial least squares regression. Remote Sensing of Environment 86(4), 542-553.

He, Y., Mui, A., 2010. Scaling up Semi-Arid Grassland Biochemical Content from the Leaf to the Canopy Level: Challenges and Opportunities. Sensors 10(12), 11072-11087.

Heitkönig, I.M.A., Owen-Smith, N., 1998. Seasonal selection of soil types and grass sward by roan antelope in a south african savanna. African Journal of Ecology 36(1), 57-70.

Hijmans, R.J., Cameron, S.E., Parra, J.L., Jones, P.G., Jarvis, A., 2005. Very High Resolution Interpolated Climate Surfaces for Global Land Areas. International Journal of Climatology 25, 1965-1978.

Hijmans, R.J., Guarino, L., Cruz, M., Rojas, E., 2001. Computer tools fro spatial anaylsis of plant genetic resources data: 1. DIVA-GIS. Plant Genetic Resources Newletter 2001(127), 15-19.

Horler, D.N.H., Dockray, M., Barber, J., 1983. The red egde of plant leaf reflectance. International Journal of Remote Sensing 4(2), 273-288.

Huang, Z., Turner, B.J., Dury, S.J., Wallis, I.R., Foley, W.J., 2004. Estimating foliage nitrogen concentration from HYMAP data using continuum removal analysis. Remote Sensing of Environment 93(1-2), 18-29.

Huete, A.R., 1988. A soil-adjusted vegetation index (SAVI). Remote Sensing of Environment 25, 295-309.

Huete, A. R., Liu, H., Q., Batchily, K. & Van Leewen, W. 1997. A comparison of vegetation indices global set of TM images for EOS-MODIS. Remote Sensing of Environment, 59 (3), 440-451.

Jain, N., Ray, S., Singh, J., Panigrahy, S., 2007. Use of hyperspectral data to assess the effects of different nitrogen applications on a potato crop. Precision Agriculture 8(4), 225-239.

James, L.F., Young, J.A., Sanders, K., 2003. A new approach to monitoring rangelands. Arid Land Research and Management 17(4), 319-318.

Javis, A., Reuter, H.I., Nelson, A., Guevara, E., 2008. The Holle-filled SRTM for the globe Version 4. Available from the CGIAR-CSI SRTM 90 m database (http://srtm.csi.cgiar.org).

Jordan, C. F. 1969. Derivation of leaf area index from quality of light on the floor. Ecology, 50, 663-666.

Knox, N.M., Skidmore, A.K., Prins, H.H.T., Asner, G.P., van der Werff, H.M.A., de Boer, W.F., van der Waal, C., de Knegt, H.J., Kohi, E.M., Slotow, R., Grant, R.C., 2011. Dry season mapping of savanna forage quality, using the hyperspectral Carnegie Airborne Observatory sensor. Remote Sensing of Environment 115(6), 1478-1488.

Knox, N.M., Skidmore, A.K., Schlerf, M., de Boer, W.F., van Wieren, S.E., van der Waal, C., Prins, H.H.T., Slotow, R., 2010. Nitrogen prediction in grasses: effect of bandwidth and plant material state on absorption feature selection. International Journal of Remote Sensing 31(3), 691-704.

Kumar, L., Schmidt, K.S., Dury, S., Skidmore, A.K., 2001. Imaging Spectroscopy and Vegetation Science, In: Van Der Meer, F.D., De Jong, S.M. (Eds.), Image Spectroscopy. Kluver Academc Publishers, Dordrecht, pp. 111-154.

LaCapra, V.C., Melack, J.M., Gastil, M., Valeriano, D., 1996. Remote sensing of foliar chemistry of inundated rice with imaging spectrometry. Remote Sensing of Environment 55(1), 50-58.

le Maire, G., Francois, C., Soudani, K., Berveiller, D., Pontailler, J.Y., Breda, N., Genet, H., Davi, H., Dufrene, E., 2008. Calibration and validation of hyperspectral indices for the estimation of broadleaved forest leaf chlorophyll content, leaf mass per area, leaf area index and leaf canopy biomass. Remote Sensing of Environment 112(10), 3846-3864.

Lehman, E., 1998. Non-parametrics: Statistical Methods Based on Ranks. Prentice-Hall, Upper Saddle River.

Main, R., Cho, M.A., Mathieu, R., O'Kennedy, M.M., Ramoelo, A., Koch, S., 2011. An investigation into robust spectral indices for leaf chlorophyll estimation. ISPRS Journal of Photogrammetry and Remote Sensing 66(6), 751-761.

Majeke, B., van Aardt, J.A.N., Cho, M.A., 2008. Imaging spectroscopy of foliar biochemistry in forestry environments. Southern Forests 70(3), 275-285.

McNaughton, S.J., 1988. Mineral nutrition and spatial concentrations of African ungulates. Nature 334, 343-345.

McNaughton, S.J., 1990. Mineral nutrition and seasonal movements of African migratory ungulates. Nature 345, 613-615.

Metternicht, G. 2003. Vegetation indices derived from high-resolution airborne videography for precision crop management. International Journal of Remote Sensing, 24 (14), 2855 - 2877.

Mucina, L., Rutherford, M.C., 2006. The Vegetation of South Africa, Lesotho and Swaziland. Strelitzia, Cape Town.

Mutanga, O., Prins, H.H.T., Skidmore, A.K., van Wieren, S., Huizing, H., Grant, R., Peel, M., Biggs, H., 2004. Explaining grass-nutrient patterns in a savanna rangeland of southern Africa. Journal of Biogeography 31(5), 819-829.

Mutanga, O., Skidmore, A.K., 2004a. Integrating imaging spectroscopy and neural networks to map grass quality in the Kruger National Park, South Africa. Remote Sensing of Environment 90(1), 104-115.

Mutanga, O., Skidmore, A.K., 2004b. Narrow band vegetation indices overcome the saturation problem in biomass estimation. International Journal of Remote Sensing 25(19), 3999 - 4014.

Mutanga, O., Skidmore, A.K., 2007. Red edge shift and biochemical content in grass canopies. ISPRS Journal of Photogrammetry and Remote Sensing 62, 34-42.

Mutanga, O., Skidmore, A.K., Van Wieren, S.E., 2003. Descriminating tropical grass (*Cenhrus ciliaris*) canopies grown under different nitrogen treatments using spectroradiometry. ISPRS Journal of Photogrammetry and Remote Sensing 57(3), 263-272.

Olff, H., Ritchie, M.E., Prins, H.H.T., 2002. Global environmental controls of diversity in large herbivores. Nature 415(6874), 901.

Owen-Smith, N., Danckwerts, J., E., 1997. Herbivory, In: Cowling, R.M., Richardson, D.M., Pierce, S.M. (Eds.), Vegetation of Southern Africa. Cambridge University Press, Cambridge.

Peñuelas, J., Fillela, I., Llolet, P., Munoz, F. & Vilajeliu, M. 1995. Reflectance assessment of mite effects on apple trees. International Journal of Remote Sensing, 16 (14), 2727-2733.

Pickett, S.T.A., Gadenasso, M.L., Benning, T.L., 2003. Biotic and Abiotic Variability as Key Determinants of Savanna Heterogeneity at Spatiotemporal Scales, In: Du Toit, J.T., Rogers, K.H., Biggs, H.C. (Eds.), The Kruger Experience: Ecology and Management of Savanna Heterogeneity. Island Press, London, pp. 22-40.

Plummer, S.E., 1988a. Exploring the relationships between leaf nitrogen content, biomass and the near-infrared/red reflectance ratio. International Journal of Remote Sensing 9(1), 177-183.

Plummer, S.E., 1988b. Relationships Between The Nitrogen Content Of Grass And Reflectance, Geoscience and Remote Sensing Symposium, 1988. IGARSS '88. Remote Sensing: Moving Toward the 21st Century., International, pp. 265-267.

Prins, H.H.T., Beekman, J., 1989. A balanced diet as a goal for grazing: The food of the manyara buffalo. African Journal of Ecology 27, 241-259.

Prins, H.H.T., van Langevelde, F., 2008. Assembling diet from different places, In: Prins, H.H.T., van Langevelde, F. (Eds.), Resource Ecology: Spatial and Temporal Dynamics of Foraging. Springer, Netherlands, pp. 129-154.

Qi, J., Chehbouni, A., Huete, A. R., Kerr, Y. H. & Sorooshian, S. 1994. A modified soil adjusted vegetation index. Remote Sensing of Environment, 48 (2), 119-126.

Ramoelo, A., Cho, M.A., Mathieu, R., Skidmore, A.K., Schlerf, M., Heitkönig, I.M.A., Prins, H.H.T., 2011a. Integrating environmental and in situ hyperspectral remote sensing variables for grass nitrogen estimation in savanna ecosystems, 34th Internation Symposium on the Remote

Sensing of Environment (ISRSE 2011), The GEOSS Era: Towards Operational Environmental Monitoring, Sydney, Australia, http://www.isprs.org/proceedings/2011/ISRSE-34/index.html , Accessed: August 2011.

Ramoelo, A., Skidmore, A.K., Cho, M.A., Mathieu, R., Heitkönig, I.M.A., Dudeni-Thlone, N., Schlerf, M., Prins, H.H.T., *under review*. Non-linear partial least square regression increases the estimation accuracy of grass nitrogen and phosphorus using in situ hyperspectral and environmental data. ISPRS Journal of Photogrammetry and Remote Sensing.

Ramoelo, A., Skidmore, A.K., Schlerf, M., Mathieu, R., Heitkönig, I.M.A., 2011b. Water-removed spectra increase the retrieval accuracy when estimating savanna grass nitrogen and phosphorus concentrations. ISPRS Journal of Photogrammetry and Remote Sensing 66(4), 408-417.

RapidEye, 2010. RapidEye Standard Image Product Specification, Version 3.0, Germany, www.rapideye.de accessed on April 2010.

Richter, R., 2011. Atmospheric/Topographic fro Satellite Imagery (ATCOR 2/3 User Guide, Version 8). DLR-German Aerospace Center, Wessling, Germany.

Roberts, B.R., 1987. The Availability of Herbage, In: Harker, J.B., Ternouth, J.H. (Eds.), The Nutrition of Herbivores. Academic Press, London, pp. 47-63.

Rondeaux, G., Steven, M. & Baret, F. 1996. Optimized of Soil-adjusted vegetation indices. Remote Sensing of Environment, 55 (2), 95-107.

Roujean, J.-L. & Breon, F.-M. 1995. Estimating PAR absorbed by vegetation from bidirectional reflectance measurements. Remote Sensing of Environment, 51 (3), 375-384.

Rouse, J.W., Haas, R.H., Schell, J.A., Deering, D.W., Harlan, J.C., 1974. Monitoring the vernal advancement and retrogradation of natural vegetation, NASA/GSFC, Type III Final Report, M.D. Greenbelt, 371.

Saad, A., Adams, D.C., Wicknick, J.A., 2007. Bioclimatic modelling, morphology, and behaviour reveal alternative mechanisms regulating the distribution of two parapatric salamander species. Evolutionary Ecology Research 9, 843-854.

Sakamoto, Y., Ishiguro, M., Kitagawa, G., 1986. Akaike Information Criteria Statistics. D. Reidel Publishing Company, US.

Schleicher, T. D., Bausch, W. C., Delgado, J. A. & Ayers, P. D. 2001. Evaluation and refinement of the nitrogen reflectance index (NRI) for site-specific fertilizer management. Paper number 011151, ASAE Annual Meeting, St. Joseph, Michigan.

Schlerf, M., Atzberger, C., Hill, J., Buddenbaum, H., Werner, W., Schüler, G., 2010. Retrieval of chlorophyll and nitrogen in Norway spruce (Picea abies L. Karst.) using imaging spectroscopy. International Journal of Applied Earth Observation and Geoinformation 12(1), 17-26.

Scholes, R.J., Bond, W.J., Eckhardt, H.C., 2003. Vegetation Dynamics in the Kruger Ecosystem, In: Du Toit, J.T., Rogers, K.H., Biggs, H.C. (Eds.), The Kruger Experience : Ecology and Management of Savanna Heterogeneity. Island Press, London.

Shackleton, S.E., Shackleton, C.M., Netshiluvhi, P.R., Geach, B.S., Ballance, A., Fairbanks, D.H.K., 2002. Use patterns and value of savanna resources in three rural villages in South Africa. Economic Botany 56(2), 130-146.

Skidmore, A.K., Ferwerda, J.G., Mutanga, O., Van Wieren, S.E., Peel, M., Grant, R.C., Prins, H.H.T., Balcik, F.B., Venus, V., 2010. Forage quality of savannas -- Simultaneously mapping foliar protein and polyphenols for trees and grass using hyperspectral imagery. Remote Sensing of Environment 114(1), 64-72.

Skidmore, A.K., Franklin, J., Dawson, T.P., Pilejso, P., 2011. Geospatial tools address emerging issues in spatial ecology: a review and commentary on the Special Issue. International Journal of Geographical Information Science 25(3), 337-365.

Smith, R. C. G., Adams, J., Stephens, D. J. & Hick, P. T. 1995. Forecasting wheat yield in a Mediterranean type of environment from the NOAA satellite. Australian Journal of Agricultural Research, 46 (1), 113-125.

Starks, P.J., Zhao, D., Brown, M.A., 2008. Estimation of nitrogen concentration and in vitro dry matter digestibility of herbage of warm-season grass pastures from canopy hyperspectral reflectance measurements. Grass Forage Sci. 63(2), 168-178.

Thenkabail, P.S., Smith, R.B., De Pauw, E., 2000. Hyperspectral vegetation indices and their relationships with agricultural crop characteristics. Remote Sensing of Environment 71(2), 158-182.

Tolsma, D.J., Ernst, W.H.O., Verweij, R.A., Vooijs, R., 1987. Seasonal Variation of Nutrient Concentrations in a Semi-Arid Savanna Ecosystem in Botswana. Journal of Ecology 75(3), 755-770.

Treydte, A.C., Heitkönig, I.M.A., Prins, H.H.T., Ludwig, F., 2007. Trees improve grass quality for herbivores in African savannas. Perspectives in Plant Ecology, Evolution and Systematics 8(4), 197-205.

Tucker, C.J., 1977. Asymptotic nature of grass canopy spectral reflectance. Applied Optics 16(57-1151).

Venter, F.J., Scholes, R.J., Eckhardt, H.C., 2003. Abiotic template and its associated vegetation pattern, In: Du Toit, J.T., Kevin, H.R., Biggs, H.C. (Eds.), The Kruger Experience: Ecology and Management of Savanna Heterogeneity. The Island Press, London.

Vos, J., Bom, M., 1993. Hand-held chlorophyll meter: a promising tool to assess the nitrogen status of potato foliage. Potato Research 36(4), 301-308.

Walczak, B., Massart, D.L., 1996. The Radial Basis Functions -- Partial Least Squares approach as a flexible non-linear regression technique. Analytica Chimica Acta 331(3), 177-185.

Wang, Z.J., Wang, J.H., Liu, L.Y., Huang, W.J., Zhao, C.J., Wang, C.Z., 2004. The prediction of grain protein in winter wheat (*Triticum aestivum*) using plant pigment ratio (PPR). Field Crops Research 90, 311-321.

Wessman, C.A., 1992. Imaging spectroscopy for remote sensing of ecosystem processes. Advances in Space Research 12(7), 361-368.

Wu, C., Niu, Z., Tang, Q. & Huang, W. 2008. Estimating chlorophyll content from hyperspectral vegetation indices: Modeling and validation. Agricultural and Forest Meteorology, 148 (8-9), 1230-1241.

Yoder, B.J., Pettigrew-Crosby, R.E., 1995. Predicting nitrogen and chlorophyll content and concentrations from reflectance spectra (400-2500 nm) at leaf and canopy scales. Remote Sensing of Environment 53(3), 199-211.

Zarco-Tejada, P.J., Miller, J.R., Morales, A., Berjon, A., Aguera, J., 2004. Hyperspectral indices and model simulation for chlorophyll estimation in open-canopy tree crops. Remote Sensing of Environment 90(4), 463-476.

Zhou, G., Wang, Y., Wang, S., 2002. Responses of grassland ecosystems to precipitation and land use along the Northeast China Transect. Journal of Vegetation Science 13(3), 361-368.

Figure 1
Click here to download high resolution image

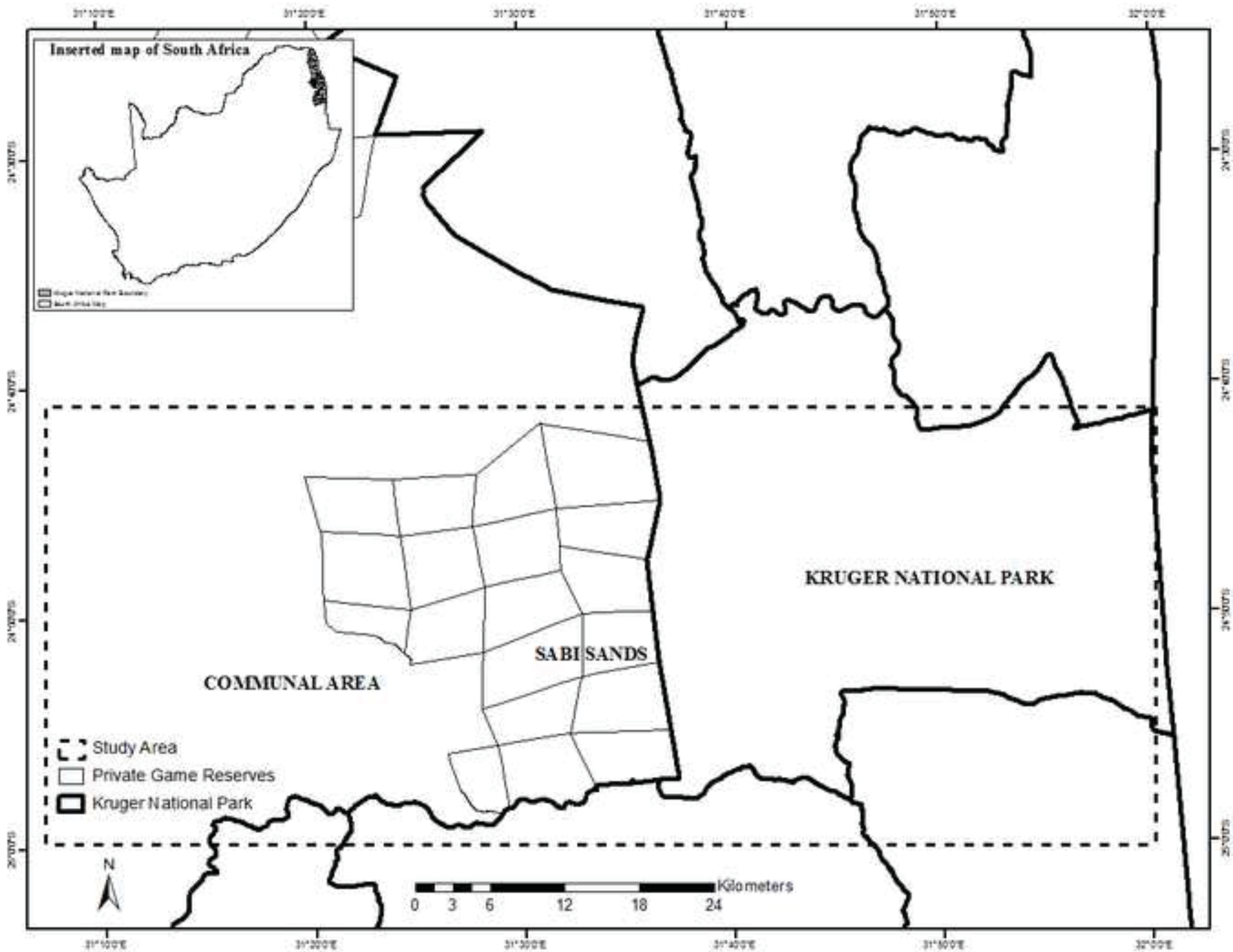

Figure 2
Click here to download high resolution image

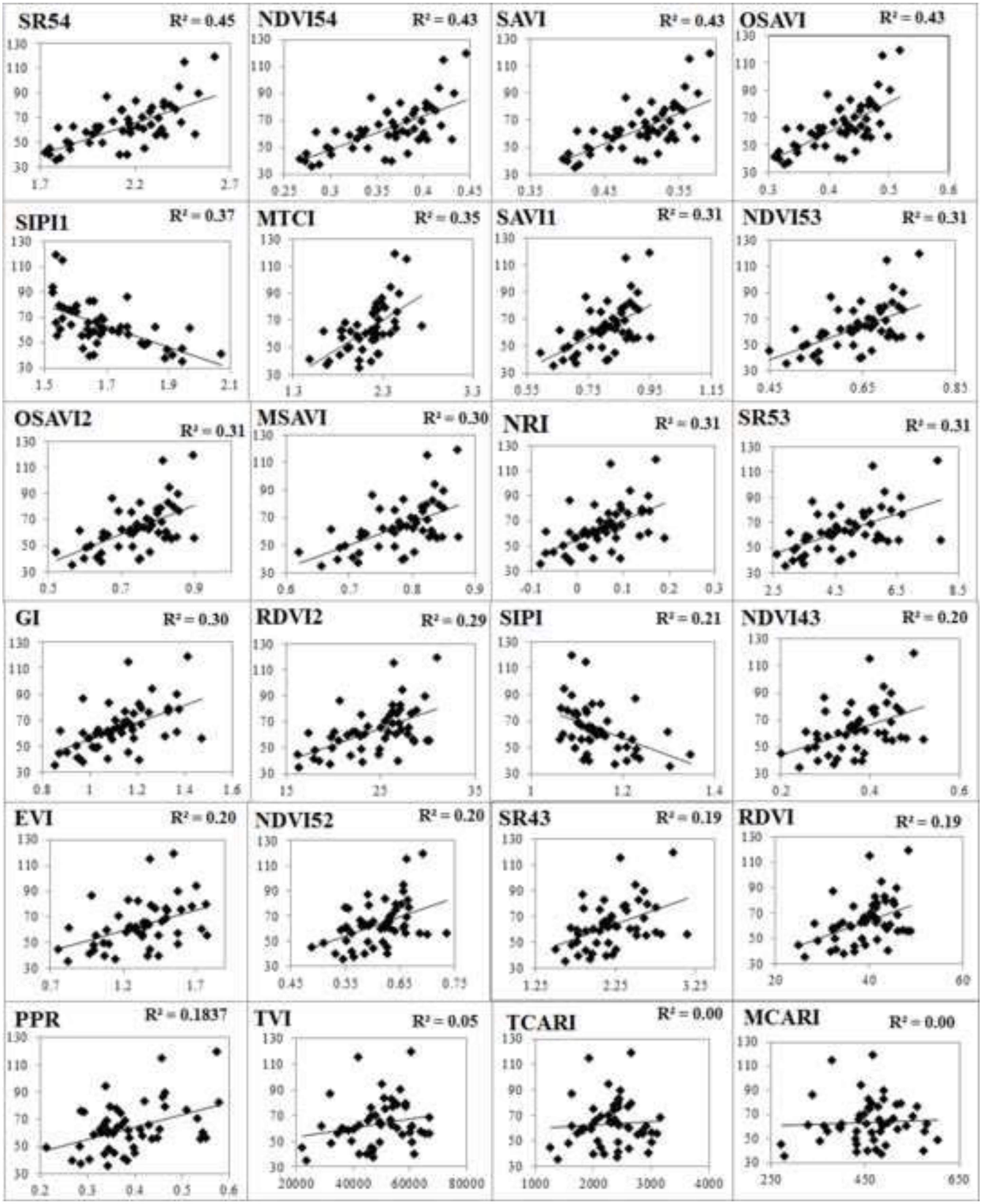

Figure 3

Click here to download high resolution image

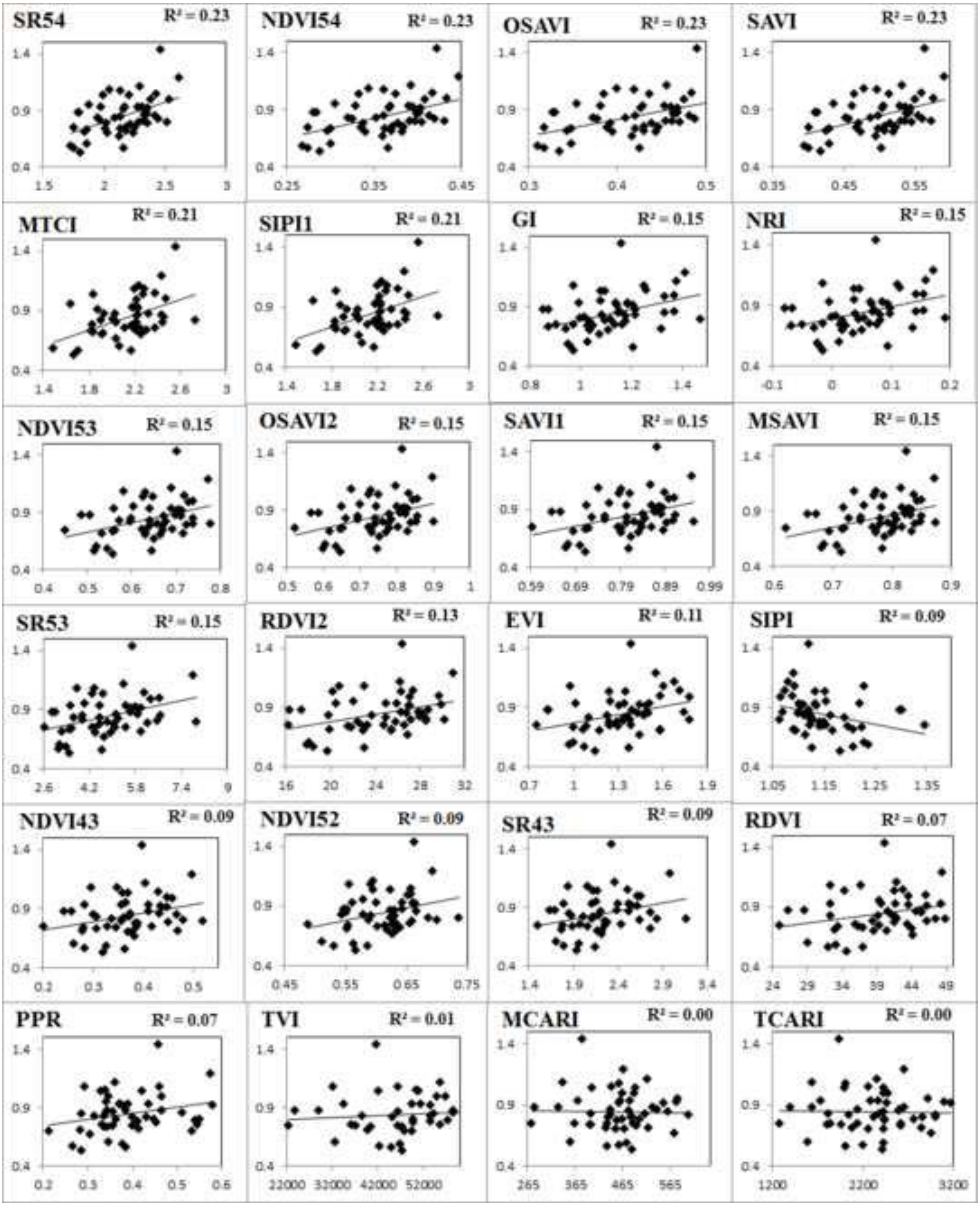

Figure 4
Click here to download high resolution image

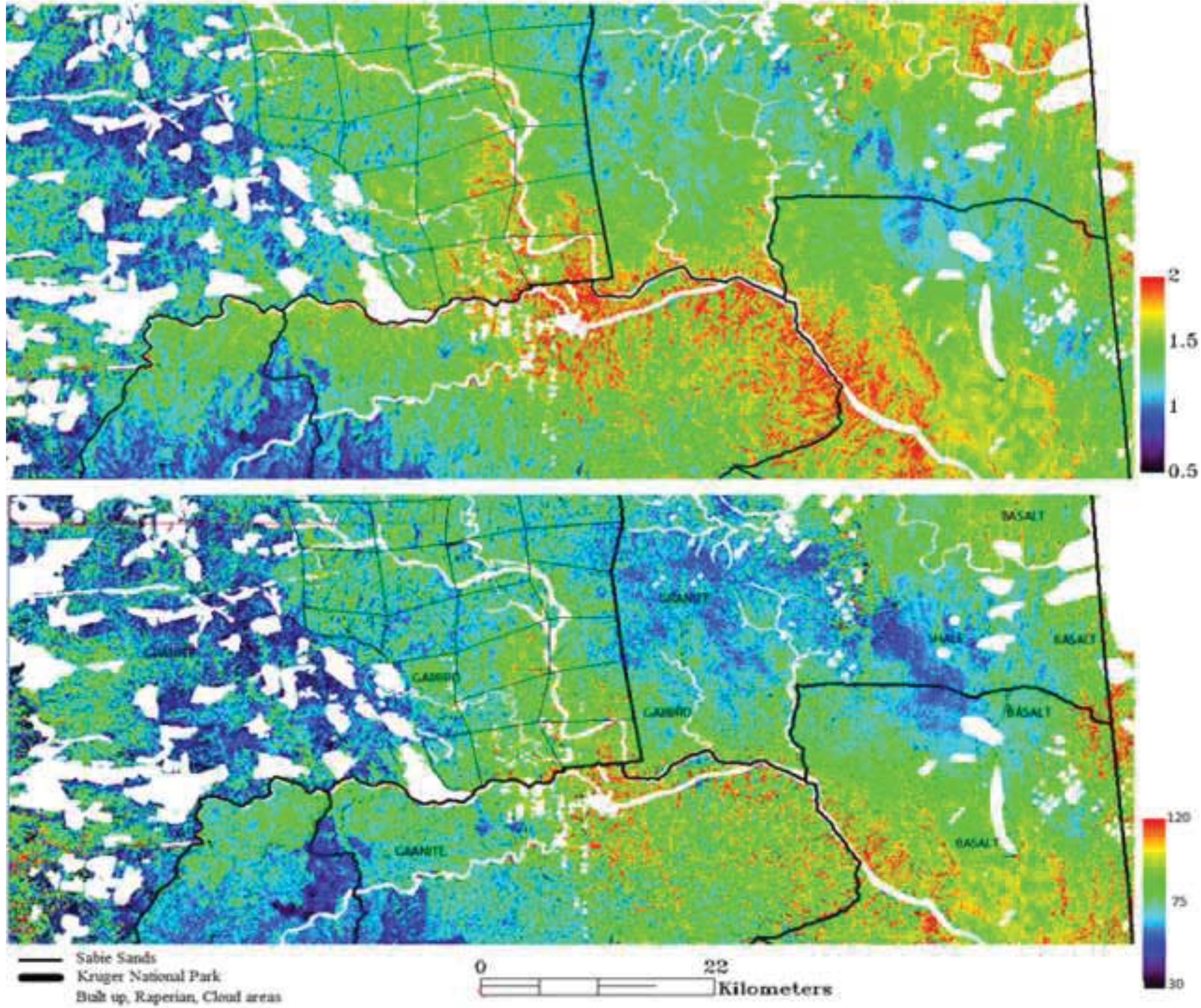

Figure 5
Click here to download high resolution image

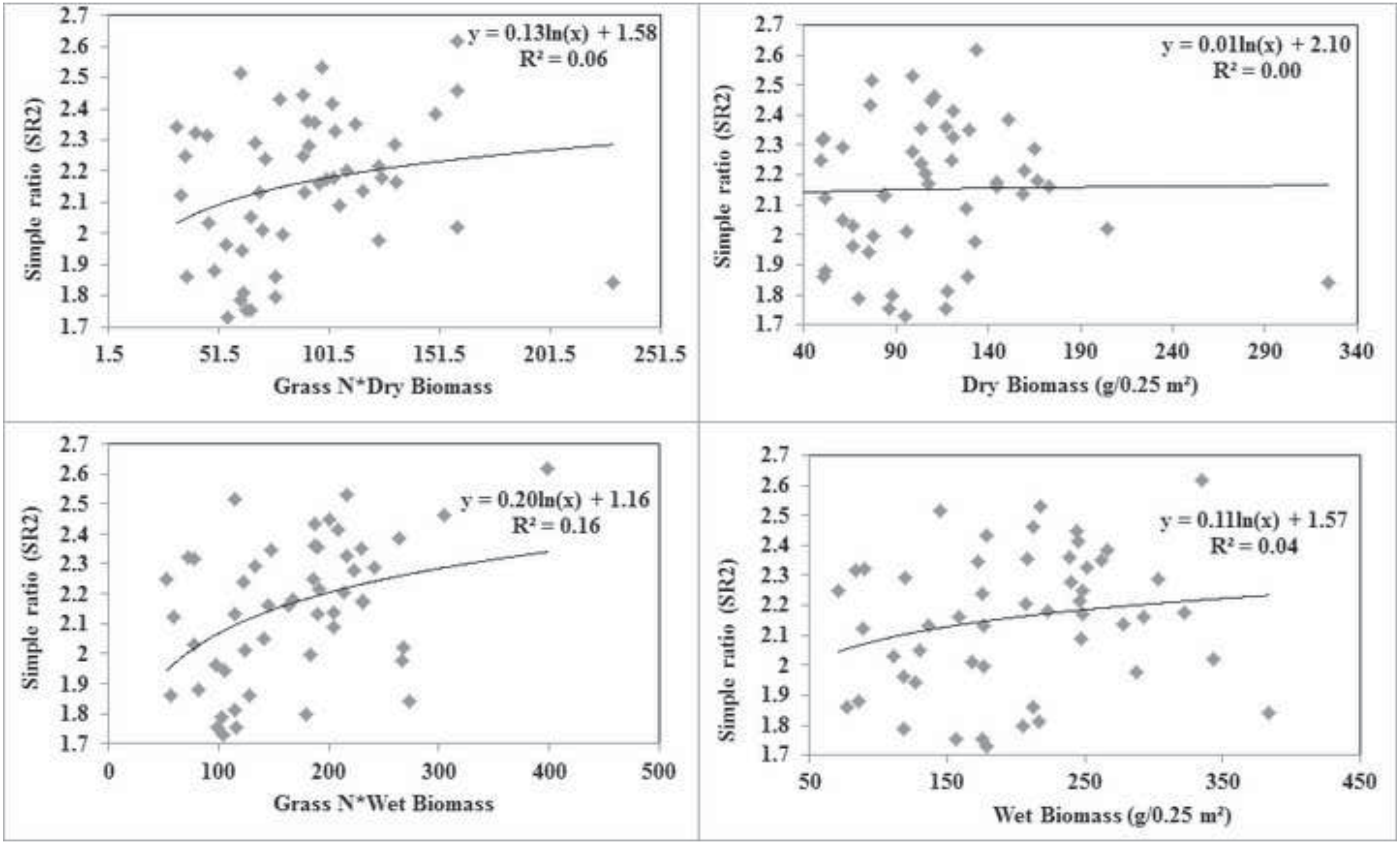

Figures' captions

Figure 1: Map of the Study area

Figure 2: Scatterplots of canopy N (N*PV) and various vegetation indices **(X-axis=vegetation index and Y-axis=N*PV)**. SR=Simple Ratio, NDVI=Normalized Difference Vegetation Index, SAVI=Soil Adjusted Vegetation Index, L=Soil Correction Factor, OSAVI=Optimized SAVI, MSAVI=Modified SAVI, TVI=Triangular Vegetation Index, RDVI=Renormalized Difference Vegetation Index, MCARI=Modified Chlorophyll Absorption Ratio Index, MTCI=MERIS Terrestrial Chlorophyll Index, PPR=Plant Pigment Ratio, NRI=Nitrogen Reflectance Index, SIPI=Structure Insensitive Pigment Index, GI=Greenness Index, EVI=Enhanced Vegetation Index, TCARI=Transformed Chlorophyll Absorption Ratio.

Figure 3: Scatterplots of foliar N (%) and various vegetation indices **(X-axis=vegetation index and Y-axis=N)**. SR=Simple Ratio, NDVI=Normalized Difference Vegetation Index, SAVI=Soil Adjusted Vegetation Index, L=Soil Correction Factor, OSAVI=Optimized SAVI, MSAVI=Modified SAVI, TVI=Triangular Vegetation Index, RDVI=Renormalized Difference Vegetation Index, MCARI=Modified Chlorophyll Absorption Ratio Index, MTCI=MERIS Terrestrial Chlorophyll Index, PPR=Plant Pigment Ratio, NRI=Nitrogen Reflectance Index, SIPI=Structure Insensitive Pigment Index, GI=Greenness Index, EVI=Enhanced Vegetation Index, TCARI=Transformed Chlorophyll Absorption Ratio.

Figure 4: Map showing the spatial distribution of the foliar N (Top) and canopy Nitrogen (N*PV) (bottom) in relation to geology classes such as basalt, gabbro, granite and shale (PV=photosynthetic vegetation cover).

Figure 5: Figure shows the saturation relationship between a vegetation index and with the interaction between N and biomass (Top Left), dry biomass (Top Right), interaction between foliar N and wet biomass (Bottom Left), and wet biomass (Bottom Right).

Tables

Table 1: Environmental variables used in this study

Environmental Data	Type	Source	Resolution
Geology	Categorical	Council for Geoscience	1:1000000
Soil	Categorical	SOTERSAF database	1:1000000
Precipitation	Continuous	http://www.worldclim.com/	1 km
Temperature	Continuous	http://www.worldclim.com/	1 km
Land use types	Categorical	KNP	Vector layer
Altitude (DEM)	Continuous	SRTM	90 m
Slope	Continuous	Derived from DEM	90 m
Aspect	Continuous	Derived from DEM	90 m
Distance from rivers	Continuous	SANBI GIS data	1:1000000

DEM= digital elevation model, CSIR=Council for Scientific and Industrial Research, SANBI=South African National Botanical Institute, SOTER=Soil and Terrain of Southern Africa database, SRTM=Shuttle Radar Topography Mission (http://srtm.csi.cgiar.org), KNP=Kruger National Park GIS datasets

Table 2: List of 24 vegetation indices used in this study

Index	Conventional Formulae	Modified Formulae	Reference
SR52	R_{NIR}/R_{RED}	$R_{805}/R_{657.5}$	(Jordan, 1969)
SR54		R_{805}/R_{710}	
SR43		$R_{710}/R_{657.5}$	
NDVI52	$(R_{NIR}-R_{RED})/(R_{NIR}+R_{RED})$	$(R_{805}-R_{555})/(R_{805}+R_{555})$	(Gitelson et al., 1996)
NDVI53		$(R_{805}-R_{657.5})/(R_{805}+R_{657.5})$	(Rouse et al., 1974)
NDVI54		$(R_{805}-R_{710})/(R_{805}+R_{710})$	
NDVI43		$(R_{710}-R_{657.5})/(R_{710}+R_{657.5})$	
SAVI	$((1+L)*R_{NIR}-R_{RED})/((R_{NIR}+R_{RED})+L)$	$((1+0.2)*R_{805}-R_{710})/((R_{805}+R_{710})+0.2)$	(Huete, 1988)
SAVI1		$((1+0.2)*R_{805}-R_{657.5})/((R_{805}+R_{657.5})+0.2)$	
OSAVI	$(1+0.16)*(R_{800}-R_{670})/(R_{800}+R_{670}+0.16)$	$(1+0.16)*(R_{805}-R_{710})/(R_{805}+R_{710}+0.16)$	(Rondeaux et al., 1996)
OSAVI2	$(1+0.16)*(R_{750}-R_{705})/(R_{750}+R_{705}+0.16)$	$(1+0.16)*(R_{805}-R_{657.5})/(R_{805}+R_{657.5}+0.16)$	(Wu et al., 2008)
MSAVI	$0.5*(2*R_{800}+1-SQRT((2*R_{800}+1)^2-8(R_{800}-R_{670})))$	$0.5*(2*R_{800}+1-SQRT((2*R_{800}+1)^2-8(R_{800}-R_{670})))$	(Qi et al., 1994)
TVI	$0.5*(120*(R_{750}-R_{550})-200*(R_{670}-R_{550}))$	$0.5*(120*(R_{710}-R_{555})-200*(R_{657.5}-R_{555}))$	(Broge and Leblanc, 2000)
RDVI	$(R_{800}-R_{670})/(SQRT(R_{800}+R_{670})$	$(R_{805}-R_{657.5})/(SQRT(R_{805}+R_{657.5})$	(Roujean and Breon, 1995)
RDVI1		$(R_{805}-R_{710})/(SQRT(R_{805}+R_{657.5})$	
MCARI	$((R_{700}-R_{670})-0.2*(R_{700}-R_{550}))*(R_{700}/R_{670})$	$((R_{710}-R_{657.5})-0.2*(R_{710}-R_{555}))*(R_{710}/R_{657.5})$	(Daughtry et al., 2000)
MTCI	$(R_{754}-R_{709})/(R_{709}-R_{681})$	$(R_{800}-R_{710})/(R_{710}-R_{657.5})$	(Dash and Curran, 2004)
PPR	$(R_{550}-R_{450})/(R_{550}+R_{450})$	$(R_{555}-R_{475})/(R_{555}+R_{475})$	(Metternicht, 2003)
NRI	$(R_{570}-R_{670})/(R_{570}+R_{670})$	$(R_{555}-R_{657.5})/(R_{555}+R_{657.5})$	(Schleicher et al., 2001)
SIPI	$(R_{800}-R_{445})/(R_{800}-R_{680})$	$(R_{805}-R_{475})/(R_{805}-R_{657.5})$	(Peñuelas et al., 1995)
SIPI1		$(R_{710}-R_{475})/(R_{710}-R_{657.5})$	
GI	(R_{554}/R_{677})	$(R_{555}/R_{657.5})$	(Smith et al., 1995)
EVI	$2.5*(R_{800}-R_{670})/R_{800}+(6*R_{670})-(7.5*R_{475})+1))$	$2.5*(R_{805}-R_{657.5})/R_{805}+(6*R_{657.5})-(7.5*R_{475})+1))$	(Huete et al., 1997)
TCARI	$3*((R_{700}-R_{670})-0.2*(R_{700}-R_{550})*(R_{700}/R_{670}))$	$3*((R_{710}-R_{657.5})-0.2*(R_{710}-R_{555})*(R_{710}/R_{657.5}))$	(Haboudane et al., 2002)

SR=Simple Ratio, NDVI=Normalized Difference Vegetation Index, SAVI=Soil Adjusted Vegetation Index, L=Soil Correction Factor, OSAVI=Optimized SAVI, MSAVI=Modified SAVI, TVI=Triangular Vegetation Index, RDVI=Renormalized Difference Vegetation Index, MCARI=Modified Chlorophyll Absorption Ratio Index, MTCI=MERIS Terrestrial Chlorophyll Index, PPR=Plant Pigment Ratio, NRI=Nitrogen Reflectance Index, SIPI=Structure Insensitive Pigment Index, GI=Greenness Index, EVI=Enhanced Vegetation Index, TCARI=Transformed Chlorophyll Absorption Ratio

Table 3: Ranking by bootstrapped root mean square error for various vegetation indices in predicting (a) Canopy Nitrogen and (b) foliar Nitrogen

Ranks	Indices (a)	RMSE	Indices (b)	RMSE (%)
1	SR54	13.5058	SR54	0.15029
2	NDVI54	13.6593	NDVI54	0.15084
3	SAVI	13.6623	OSAVI	0.15090
4	OSAVI	13.6668	SAVI	0.15099
5	SIPI1	14.4088	MTCI	0.15307
6	MTCI	14.7138	SIPI1	0.15321
7	SAVI1	15.0803	GI	0.15793
8	NDVI53	15.0875	NRI	0.15815
9	OSAVI2	15.1051	NDVI53	0.15821
10	MSAVI	15.1245	OSAVI2	0.15837
11	NRI	15.1576	SAVI1	0.15838
12	SR53	15.2035	MSAVI	0.15852
13	GI	15.2318	SR53	0.15856
14	RDVI2	15.3076	RDVI2	0.16025
15	SIPI	16.1433	EVI	0.16131
16	NDVI43	16.2270	SIPI	0.16340
17	EVI	16.2315	NDVI43	0.16340
18	NDVI52	16.3093	NDVI52	0.16354
19	SR43	16.3612	SR43	0.16393
20	RDVI	16.3641	RDVI	0.16510
21	PPR	16.4510	PPR	0.16595
22	TVI	17.6611	TVI	0.17040
23	TCARI	18.0888	MCARI	0.17120
24	MCARI	18.1006	TCARI	0.17137

SR=Simple Ratio, NDVI=Normalized Difference Vegetation Index, SAVI=Soil Adjusted Vegetation Index, *L*=Soil Correction Factor, OSAVI=Optimized SAVI, MSAVI=Modified SAVI, TVI=Triangular Vegetation Index, RDVI=Renormalized Difference Vegetation Index, MCARI=Modified Chlorophyll Absorption Ratio Index, MTCI=MERIS Terrestrial Chlorophyll Index, PPR=Plant Pigment Ratio, NRI=Nitrogen Reflectance Index, SIPI=Structure Insensitive Pigment Index, GI=Greenness Index, EVI=Enhanced Vegetation Index, TCARI=Transformed Chlorophyll Absorption Ratio.

Table 4: The performance of various multivariate techniques used validated by bootstrapping

	R^2	**RMSE**	**RMSE(% of Mean)**	***p*-value**	**Selected variables**
Canopy N					
SMLR+PCA	0.56	12.33	16.50	<0.05	PC1, PC3, PC9
SMLR+Raw	0.59	11.60	15.52	<0.05	SR54, Altitude
RBF-PLSR	0.61	11.00	14.72	<0.05	4 factors, and 0.7 Sigma value
SMLR+Raw+Int.	0.64	11.00	14.72	<0.05	SR54, Altitude, SR54*Altitude
Foliar N		RMSE (%)			
SMLR+PCA	0.45	0.14	16.66	<0.05	PC1-4, PC9, PC10
SMLR+Raw	0.44	0.13	15.47	<0.05	SR54, Altitude, Aspect, Dist
RBF-PLSR	0.48	0.12	14.28	<0.05	5 Factors, and 1 Sigma value

SMLR=Stepwise linear regression, PCA=principal component analysis, RBF-PLSR=partial least square regression with radial basis function, SR54=simple ratio, Dist=distance to rivers, Raw=SR54 and environmental variables used as they are. Int.=indicates a model with the interaction effects of the variables significantly selected in SMLR+Raw.
p value at the 95% confidence level ($p<0.05$).

Table 5: Spearman *p* correlation matrix between N and various environmental or ancillary variables

	N*PV	SR54	Geo	Soil	Prec	Tem	Asp	Alt	Slo	Lan	Dist
N*PV	1	**0.62**	-0.20	-0.09	**-0.37**	**0.42**	**0.20**	**0.56**	**-0.23**	**-0.50**	**-0.01**
SR54		1	-0.11	0.12	-0.06	0.12	0.06	-0.23	-0.15	-0.19	-0.09
Geo			1	**-0.35**	**0.57**	-0.14	**-0.36**	**0.31**	-0.05	**0.40**	**-0.60**
Soil				1	**-0.32**	-0.10	-0.09	0.05	0.07	-0.11	0.34
Prec					1	**-0.45**	**-0.32**	**0.63**	**0.27**	**0.76**	**0.40**
Tem						1	0.01	**-0.77**	**-0.47**	**-0.54**	-0.15
Asp							1	**-0.32**	0.22	**-0.31**	0.27
Alt								1	**0.44**	**0.78**	-0.18
Slo									1	**0.37**	0.07
Lan										1	-0.26
Dist											1

N*PV=Nitrogen*Photosynthetic vegetation cover, SR54=simple ratio, Geo=Geology, Prec=precipitation, Temp=temperature, Asp=Aspect, Alt=Altitude, Slo=Slope, Lan=Land use, Dist=distance to rivers. The **bold values** indicates that the correlation is significant at 95% confidence level ($p<0.05$).

Table 6: Descriptive statistics of the data used

Variables (%)	Minimum	Maximum	Mean	Standard deviation	Coefficient of variation
Nitrogen	0.53	1.44	0.84	0.17	0.20
PV	40.00	100.00	74.71	11.42	0.15
N* PV	35.00	119.00	63.45	17.95	0.28

PV=photosynthetic vegetation cover, N*PV=Nitrogen*PV (Canopy N)